

Phases of three dimensional large N QCD on a continuum torus

R. Narayanan

Department of Physics, Florida International University, Miami, FL 33199, USA
E-mail: rajamani.narayanan@fiu.edu

H. Neuberger

Rutgers University, Department of Physics and Astronomy, Piscataway, NJ 08855, USA
E-mail: neuberger@physics.rutgers.edu

F. Reynoso

Department of Physics, Florida International University, Miami, FL 33199, USA
E-mail: freyn001@fiu.edu

ABSTRACT: It is established by numerical means that continuum large N QCD defined on a three dimensional torus can exist in four different phases. They are (i) confined phase; (ii) deconfined phase; (iii) small box at zero temperature and (iv) small box at high temperatures.

KEYWORDS: Large N QCD, Lattice Gauge Field Theories.

Contents

1. Introduction.	1
2. Technical details	2
2.1 Lattice gauge action	2
2.2 Determination of the critical sizes	3
2.3 Lattice bulk transition	3
2.4 An order parameter	3
3. Transitions in Polyakov loops	4
3.1 Details of the data analysis	4
3.2 0c-1c transition	5
3.3 1c-2c transition on L^3 lattices	5
3.4 2c-3c transition on L^3 lattices	5
3.5 Phase diagram for $l_x \leq l_y \leq l_z$	6
4. Conclusions	6

1. Introduction.

Yang Mills theory on an l^d continuum torus ($d > 2$) exhibits a phenomenon referred to as continuum reduction whereby the theory for $l > l_1 > 0$ is independent of l ¹ [1, 2]. At $l = l_1$, the theory goes from the confined phase (0c: $l > l_1$) to the deconfined phase (1c: $l < l_1$). The order parameter is the Polyakov loop and rotational symmetry is spontaneously broken. More phases were conjectured to exist [2] in the continuum theory and these are referred to as Xc phase with $X = 2, \dots, d$.

The aim of this paper is to numerically establish the existence of the 2c and 3c phase in addition to the 0c and 1c phase for the continuum Yang-Mills theory on a periodic torus. We will use the Polyakov loop to define an order parameter to be labeled, P [3], and it will take values in the range $[0, 0.5]$. If the $U(1)$ symmetry² under which the Polyakov loop transforms non-trivially is spontaneously broken, then $\bar{P} < 0.5$. Let $\bar{P}_{x,y,z}$, be the order parameters in the three directions. Then, $\bar{P}_x = \bar{P}_y = \bar{P}_z = 0.5$ in the 0c phase.

There are three possibilities for the 1c phase and one of them is characterized by $\bar{P}_y = \bar{P}_z = 0.5$ and $\bar{P}_x < 0.5$ with rotational symmetry still present in the (y, z) plane. It is difficult to numerically establish the order of the transition from the 0c to 1c phase and we will leave it unresolved in this paper.

¹We use l_1 to denote the critical size as opposed to l_c since we will have a sequence of critical sizes.

²The $U(1)$ symmetry is the limit of the Z_N symmetry as $N \rightarrow \infty$.

The 2c phase also has three possibilities and one of them is characterized by $\bar{P}_x = \bar{P}_y < 0.5$ and $\bar{P}_z = 0.5$ with rotational symmetry present in the (x, y) plane. This transition occurs when $l = l_2 < l_1$. One can argue that the 1c to 2c phase transition is first order as follows. In the 1c phase, \bar{P}_x was less than 0.5 and \bar{P}_y was 0.5. Since $\bar{P}_x = \bar{P}_y$ in the 2c phase, it is necessary for at least \bar{P}_x or \bar{P}_y to change discontinuously at the 1c to 2c transition. If one operator shows a discontinuity, all operators will generically show discontinuities and this signals a first order transition.

Rotational symmetry is restored in the 3c phase and $\bar{P}_x = \bar{P}_y = \bar{P}_z < 0.5$. For the same reason as above, we expect the 2c to 3c phase transition to be of first order. This transition occurs when $l = l_3 < l_2$.

The 2c phase is characterized by two short directions and one infinitely long direction since the theory will not depend on the length of the direction where the U(1) is not broken. Therefore, this phase describes large N QCD in a small box at zero temperature (or infinite time). Confinement cannot be addressed in the 2c phase since we do not have large Wilson loops. The 3c phase describes large N QCD in a small box at high temperatures. The 2c to 3c transition is like the transition seen in perturbation theory on $S^2 \times S^1$ [4] where S^2 replaces the two torus along which the U(1) symmetry is broken in the 2c phase.

We extend our discussion to include $l_x \times l_y \times l_z$ torus with $l_x < l_y < l_z$. The transition from 0c to 1c will occur at $l_x = l_1$ and this is independent of l_y and l_z . The transition from 1c to 2c will occur at $l_y = l_2(l_x)$ with $0 \leq l_x \leq l_2$. Furthermore, $l_2(l_2) = l_2$ and our numerical results will show that $l_2(0) > 0$. Finally, there is no dependence on l_z . Continuing along the same lines, we can say that the 2c to 3c transition occurs at $l_z = l_3(l_x, l_y)$ with $l_3 = l_3(l_3, l_3)$. It is possible that one can obtain this critical size for small l_x and l_y by perturbation theory but it is necessary to consider the zero momentum modes of the gauge fields on all three directions. We do not address this problem in the paper.

The results in this paper complement the results in the closely related paper by Bursa and Teper [5]. We mainly focus on the continuum limit of the various phases using Polyakov loops. The paper is organized as follows. We define the relevant technical details in section 2. Our numerical results showing the existence of the various phases are presented in section 3.

2. Technical details

2.1 Lattice gauge action

We used the single plaquette Wilson action given by

$$S = \frac{\beta}{4N} \sum_{x, i \neq j} \text{Tr}[U_{ij}(n) + U_{ij}^\dagger(x)] \quad (2.1)$$

$$U_{ij}(n) = U_i(n)U_j(n + \hat{i})U_i^\dagger(n + \hat{j})U_j^\dagger(n) \quad (2.2)$$

n is a three component integer vector labeling the site, i labels a direction and \hat{i} denotes a unit vector in the i direction. The link matrices $U_\mu(n)$ are in $SU(N)$. We define

$$b = \frac{\beta}{2N^2} \quad (2.3)$$

and take the large N limit with b held fixed.

All computations were done on a $L_x \times L_y \times L_z$ periodic lattice with $L_x \leq L_y = L_z$. One gauge field update of the whole lattice [2] is one Cabibo-Marinari heat-bath update of the whole lattice followed by one SU(N) over-relaxation update of the whole lattice. The code was run on two clusters, one with 48 nodes and another with 31 nodes. The nodes in the cluster were simply used to generate more statistics using a parallel random number generator and generating independent configurations with the same set of parameters on different nodes.

2.2 Determination of the critical sizes

Given the lattice coupling b and lattice sizes L_x and L_y , the dimensionless physical sizes are defined as

$$l_{x,y} = \lim_{b \rightarrow \infty} L_{x,y}/b_{\text{tad}}. \quad (2.4)$$

The tadpole improved coupling [6], b_{tad} is defined as

$$b_{\text{tad}} = be(b) = b \left\langle \frac{1}{12NL_xL_yL_z} \sum_{n,i \neq j} \text{Tr}[U_{ij}(n) + U_{ij}^\dagger(n)] \right\rangle \quad (2.5)$$

2.3 Lattice bulk transition

Since the computations in this paper use the Wilson gauge action on the lattice, it is necessary to address the unphysical transition which is the extension of the Gross-Witten transition [7] in QCD₂. The order parameter for this transition is the plaquette operator. The third order transition analytically computed in QCD₂ remains to be true based on a numerical investigation in QCD₃ [5] and the critical point is $b = 0.43$. This lattice transition does not survive the continuum limit and we will work with $b > 0.43$ throughout this paper in order to describe continuum physics.

2.4 An order parameter

An order parameter suitable for studying the phase transitions we are interested in is [3]

$$\begin{aligned} \bar{P}_{x,y,z} &= \langle P_{x,y,z} \rangle \\ P_{x,y,z} &= \frac{1}{2L_xL_yL_z} \sum_n \left(1 - \left| \frac{1}{N} \text{Tr} \mathcal{P}_{x,y,z}(n) \right|^2 \right) \\ \mathcal{P}_{x,y,z}(n) &= \prod_{m=1}^{L_{x,y,z}} U_i(n + m\hat{i}). \end{aligned} \quad (2.6)$$

The quantity $P_{x,y,z}$ takes values in the range $[0, 0.5]$ on any gauge field background and we choose the x , y and z directions on each configuration such that $P_x < P_y < P_z$.

Although this observable needs to be renormalized, we found it sufficient to work with the unrenormalized operator and we also did not have to smear the link variables. The eigenvalues, $e^{i\theta_k}$; $k = 1, \dots, N$, of the Polyakov loop operator, $\mathcal{P}_{x,y,z}(n)$, are gauge invariant. $P_{x,y,z} = 0.5$ implies a uniform distribution of the eigenvalues of $\mathcal{P}_{x,y,z}(n)$. A departure from $P_{x,y,z} = 0.5$ implies the presence of a peak in the distribution of the eigenvalues of

$\mathcal{P}_{x,y,z}(n)$ and a breaking of Z_N symmetry associated with this operator. There is no gap in the distribution of the eigenvalues of $\mathcal{P}_{x,y,z}$ when Z_N is broken.

3. Transitions in Polyakov loops

All computations were done using $N = 47$. Having picked a lattice size $L_x \times L_y \times L_z$, each run listed in Table 1 was a closed loop in the lattice coupling b . The third column in Table 1 shows the range of b and the step size in b . The fourth column, N_t , shows the number of thermalization sweeps at the two end points. Only one measurement was done per node at each b and the fifth column, N_b , shows the number of sweeps done at each intermediate b before the measurement. For example, the run on 3^3 lattice, started at a $b = 0.5$ and went up to a $b = 2.5$. A total of 2000 sweeps were performed at $b = 0.5$ and $b = 2.5$ and a total of 1000 sweeps were performed for all b in between 0.5 and 2.5. The step size in b was 0.05 and this code was run on the 31 node cluster with one measurement at each b per node. All values of b between 0.5 and 2.5 had two sets of measurements; one on the way up in b and one the way down in b .

L_x	L_y	b	N_t	N_b	N_{cfg}	$\frac{L_x}{b_{\text{tad}}}(0c - 1c)$	$\frac{L_y}{b_{\text{tad}}}(1c - 2c)$	$\frac{L_z}{b_{\text{tad}}}(2c - 3c)$
3	3	[0.5,2.5;0.05]	2000	1000	31	6.14(33)	4.02(14)	2.27(17)
4	4	[0.5,3.5;0.05]	3000	600	48	5.76(21)	3.83(28)	2.14(17)
5	5	[0.5,2.5;0.05]	2000	400	31	5.60(47)	3.73(35)	2.17(23)
6	6	[0.5,4.5;0.10]	2000	400	31	5.37(48)	3.82(70)	1.99(38)
5	6	[1.5,3.5;0.10]	3000	600	48		2.70(25)	
4	5	[0.5,3.5;0.05]	3000	600	48	6.00(46)	2.47(23)	
3	4	[0.5,2.5;0.05]	3000	600	48	6.56(76)	2.07(20)	
4	6	[2.0,5.0;0.10]	3000	600	48		1.78(17)	
3	5	[2.0,4.0;0.10]	3000	600	48		1.53(15)	
3	6	[2.0,8.0;0.20]	2000	400	31		1.14(11)	

Table 1: The parameters of all the runs used to study the transitions in Polyakov loops along with the results for the critical sizes.

3.1 Details of the data analysis

The plaquette as defined in (2.5) was measured on all configurations and this was used to obtain the tadpole improved coupling, b_{tad} . Figure 1 shows the results for all three Polyakov loop observables as a function of $\frac{4}{b_{\text{tad}}}$ for the data obtained on the 4^3 lattice (second row in Table 1). The hysteresis is clear in both \bar{P}_x and \bar{P}_y for the 1c-2c transition and it is seen in all the $\bar{P}_{x,y,z}$ for the 2c-3c transition. The critical size for the various transitions along with the error is obtained by locating the two points (one for upward direction and the second for the downward direction) where the error is largest in the observable that is broken. The vertical lines in Figure 1 shows the critical sizes along with the errors and these results are shown in the last three columns of Table 1.

Within the 2c phase one sees a difference in \bar{P}_x and \bar{P}_y . But this is just a consequence of our choice of observable. Note that we have picked $P_x < P_y$ on every configuration. If we assume two independent Gaussian random variables, α and β , that have the same mean and variance, then one can show that the variables P_x and P_y defined as the minimum and maximum of α and β will be distributed such that

$$\frac{\bar{P}_y - \bar{P}_x}{\sqrt{\langle P_{x,y}^2 \rangle - P_{x,y}^2}} = \frac{2}{\sqrt{\pi - 1}}. \quad (3.1)$$

Our data within the 2c phase is consistent with the above equation.

We did not choose a range in b such that all transitions are seen on all L_x, L_y pairs since some of them were used only to investigate the 1c-2c transition. But, we always picked a range such that the end points are in one of the four phases.

3.2 0c-1c transition

Let us focus on the seventh column in Table 1 to study the confinement-deconfinement transition. The results on $3^3, 4^3, 5^3$ and 6^3 show that the 0c-1c transition is physical since the critical size, $\frac{L_x}{b_{\text{tad}}}$, is the same on all four lattices within errors. The results here are consistent with the older results presented in [1]. We also studied the 0c-1c transition on 4×5^2 and 3×4^2 and found that the critical size is independent of L_y as expected. Figure 2 shows that the six results for the 0c-1c transition do scale properly and we estimate the continuum critical size to be $l_1 = 5.90(47)$. If we take the central value for the dimensionless string tension from [8], namely, $\sqrt{\sigma} = 0.1975$, then we get

$$\frac{1}{l_1 \sqrt{\sigma}} = 0.86(7) \quad (3.2)$$

and this is consistent [9] with saying that $\frac{1}{l_1}$ is the deconfinement temperature.

3.3 1c-2c transition on L^3 lattices

The physical size associated with the 1c-2c transition, l_2 , is expected to depend on l_x , the temperature in the deconfined phase. We first estimate the critical size on lattices with $L_x = L_y$. We use the data on $3^3, 4^3, 5^3$ and 6^3 . The four results show continuum scaling as can be seen from Figure 3 and we conclude that the 1c-2c transition exists in the continuum limit. We estimate $l_2(l_2) = 3.85(43)$. As mentioned before, 1c phase is the deconfined phase. The system is a small finite box at zero temperature in the 2c phase. This transition occurs on a l^3 torus when the temperature is $1.53(21)$ times the deconfinement temperature.

3.4 2c-3c transition on L^3 lattices

We also investigated the 2c-3c transition on $3^3, 4^3, 5^3$ and 6^3 . Here again, the four results show continuum scaling as can be seen from Figure 4 and we conclude that the 2c-3c transition also exists in the continuum limit. The transition size will depend on l_x and l_y when both of them are smaller than l_z . But, we only estimate $l_3(l_3, l_3) = 2.14(26)$ here.

Large N QCD on a very small torus, l^3 , for $l < l_3$ feels the size of the box and the temperature is high. Large N QCD is in a small box of size l at zero temperature if $l > l_3$ and it undergoes a phase transition into the deconfined phase when the box size is 1.80(30) times l_3 .

3.5 Phase diagram for $l_x \leq l_y \leq l_z$

The single scale in the 1c phase is l_x which can also be thought of as inverse temperature in the deconfined phase. The 2c phase has two scales, namely the size of the two dimensional box l_x and l_y with $l_x \leq l_y$. If $l_y > l_2(l_x)$, then the theory does not depend on l_y and we are in the deconfined phase. We considered the special case of $l_x = l_y$ in section 3.3. We extended this to the case when $l_x < l_y$. For this purpose, we considered the lattices listed in last six rows of Table 1. The phase transition in \bar{P}_y is shown in Figure 5. There is an obvious dependence of the critical size l_2 on l_x .

Figure 6 summarizes the various phases by focusing on the (l_x, l_y) plane at $l_z = l_y$. The dependence of $l_2(l_x)$ is shown using the shaded square points in Figure 6. The dashed line is a quadratic fit to the seven points and we note that $l_2(0) > 0$. In order to get an overall picture, we have also shown the 0c-1c transition in Figure 6. The dotted line indicates that the 0c-1c transition does not depend on l_y for $l_y > l_x$. Figure 6 also shows the 0c, 1c and 2c phases for $l_x \leq l_y \leq l_z$. For completeness, we have also shown the 2c-3c transition as seen on this specific (l_x, l_y) plane restricted to $l_x = l_y$. Like the 1c-2c transition, the 2c-3c transition will also show a dependence on l_x for $l_x < l_y$ and the 2c phase will not reach the $l_x = l_y$ line for $l_x = l_y < l_2$. Furthermore, the 2c-3c transition curve will change as one changes the l_z that defines the (l_x, l_y) plane. We have not investigated these details pertaining to the 2c-3c transition in this paper. But, we should remark that the rest of the phase diagram does not depend on l_z for $l_z > l_y > l_x$.

4. Conclusions

Large N QCD in three dimensions on a l^3 continuum torus exists in four different phases. The theory is in the confined phase (0c) for $l \geq 5.90(47) = l_1$ and physics does not depend on the box size. This critical size is the inverse of the deconfinement temperature, $T_c = \frac{1}{l_1}$, and the theory is in the deconfined phase (1c) for $1 < \frac{T}{T_c} < 1.53(21)$.

The system is in a finite box and feels the effect of temperature (3c phase) when $l < 2.14(26) = l_3$. The temperature has no effect if $1 < \frac{l}{l_3} < 1.80(30)$ (2c phase). The system goes into the deconfined phase if $\frac{l}{l_3} > 1.80(30)$.

All phase transitions are most likely first order in nature. We have provided arguments for this scenario when going from 1c-2c and 2c-3c. Previous results [9, 10] indicate that the deconfinement phase transition is also first order.

The 1c to 2c transition on a $l_x \times l_y \times l_z$ torus with $l_x \leq l_y \leq l_z$ depends on l_x . The critical line is given by $l_2(l_x) = 0.56 + 1.08l_x - 0.059l_x^2$ and this is valid for $0 \leq l_x \leq 3.85(23)$ and it is independent of l_z . This transition has been analyzed for one point on the (l_x, l_y) plane in [5] and we are in agreement with the result in that paper.

Acknowledgments

R. N. and F.R. acknowledge partial support by the NSF under grant number PHY-055375. R.N. also acknowledges partial support from Jefferson Lab. The Thomas Jefferson National Accelerator Facility (Jefferson Lab) is operated by the Southeastern Universities Research Association (SURA) under DOE contract DE-AC05-84ER40150. H. N. acknowledges partial support by the DOE under grant number DE-FG02-01ER41165 at Rutgers, an Alexander von Humboldt award and the hospitality of the Physics department at Humboldt University, Berlin.

References

- [1] R. Narayanan and H. Neuberger, Phys. Rev. Lett. **91**, 081601 (2003) [arXiv:hep-lat/0303023].
- [2] J. Kiskis, R. Narayanan and H. Neuberger, Phys. Lett. B **574**, 65 (2003) [arXiv:hep-lat/0308033].
- [3] G. Bhanot, U. M. Heller and H. Neuberger, Phys. Lett. B **113**, 47 (1982).
- [4] K. Papadodimas, H. H. Shieh and M. Van Raamsdonk, arXiv:hep-th/0612066.
- [5] F. Bursa and M. Teper, Phys. Rev. D **74**, 125010 (2006) [arXiv:hep-th/0511081].
- [6] G. P. Lepage, arXiv:hep-lat/9607076.
- [7] D. J. Gross and E. Witten, Phys. Rev. D **21**, 446 (1980).
- [8] B. Bringoltz and M. Teper, Phys. Lett. B **645**, 383 (2007) [arXiv:hep-th/0611286].
- [9] J. Little and M. Teper, PoS **LAT2005**, 188 (2006) [arXiv:hep-lat/0509082].
- [10] P. de Forcrand and O. Jahn, Nucl. Phys. Proc. Suppl. **129**, 709 (2004) [arXiv:hep-lat/0309153]; K. Holland, JHEP **0601**, 023 (2006) [arXiv:hep-lat/0509041].

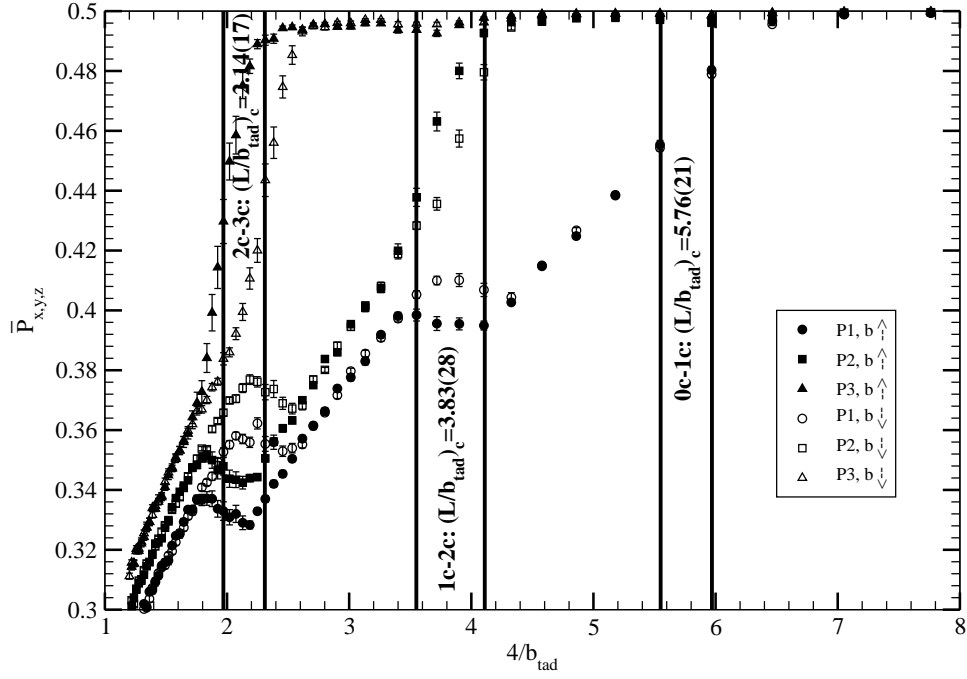


Figure 1: Plot of $\bar{P}_{x,y,z}$ for the data in the second row of Table 1 showing all three transitions.

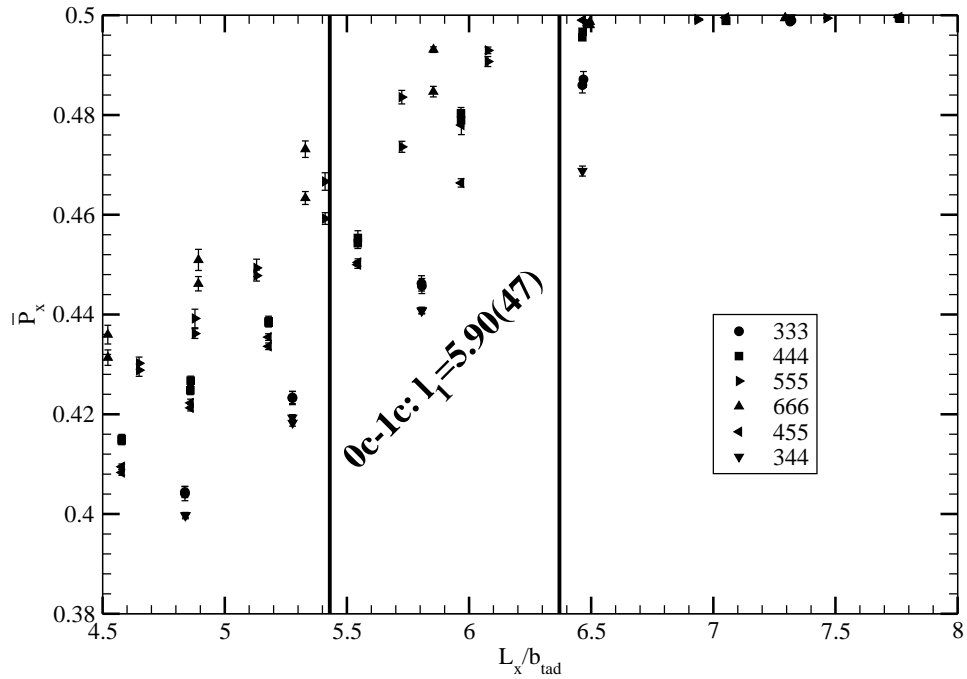


Figure 2: Plot of \bar{P}_x showing the 0c-1c transition.

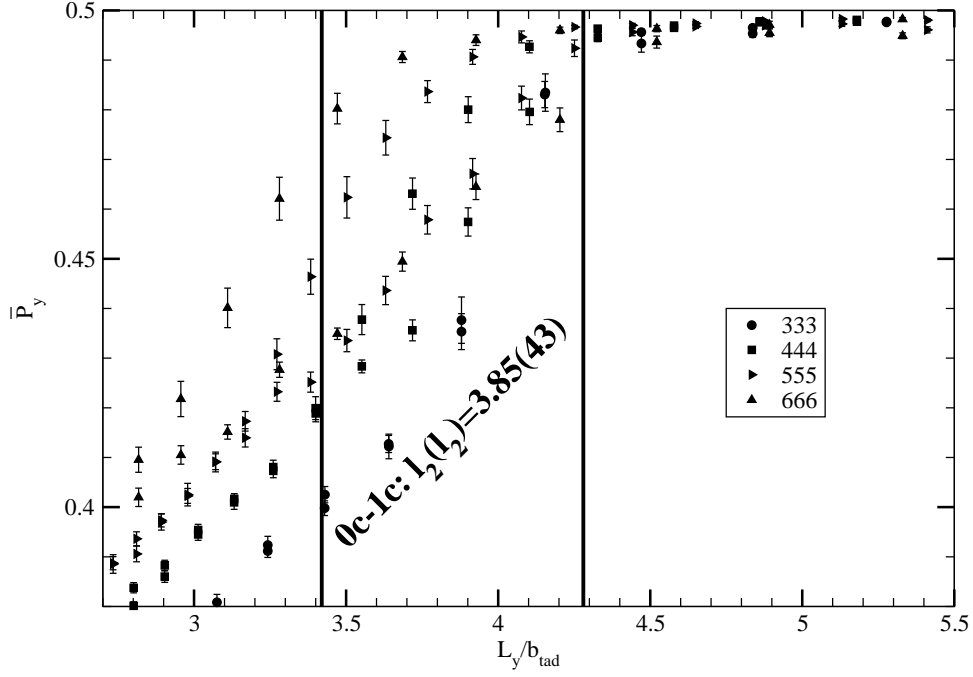


Figure 3: Plot of \bar{P}_y showing the 1c-2c transition on lattices with $L_x = L_y$.

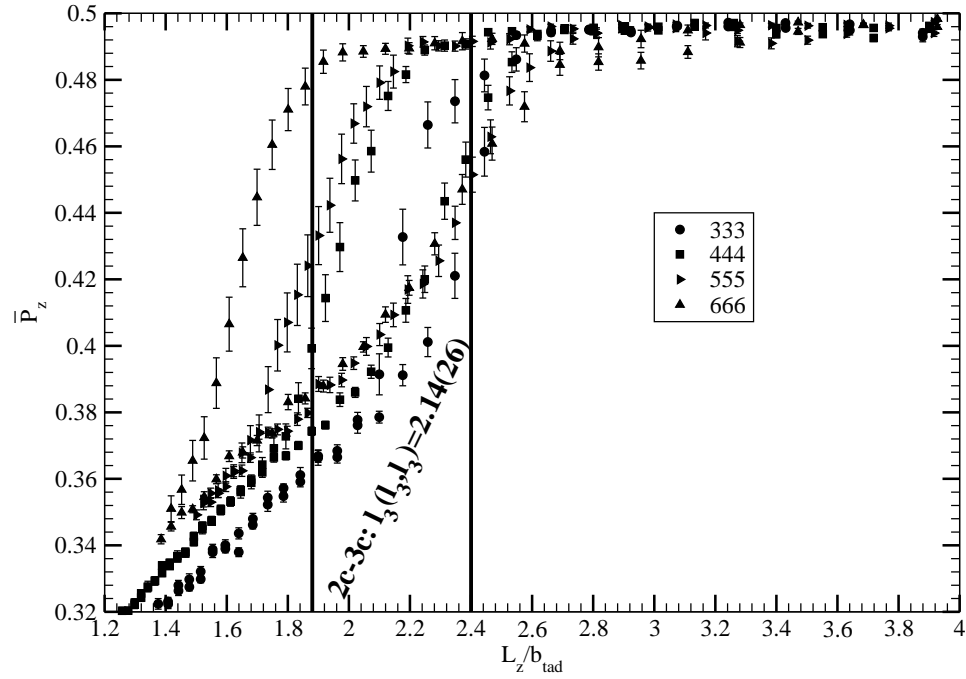


Figure 4: Plot of \bar{P}_z showing the 2c-3c transition on lattices with $L_x = L_y$.

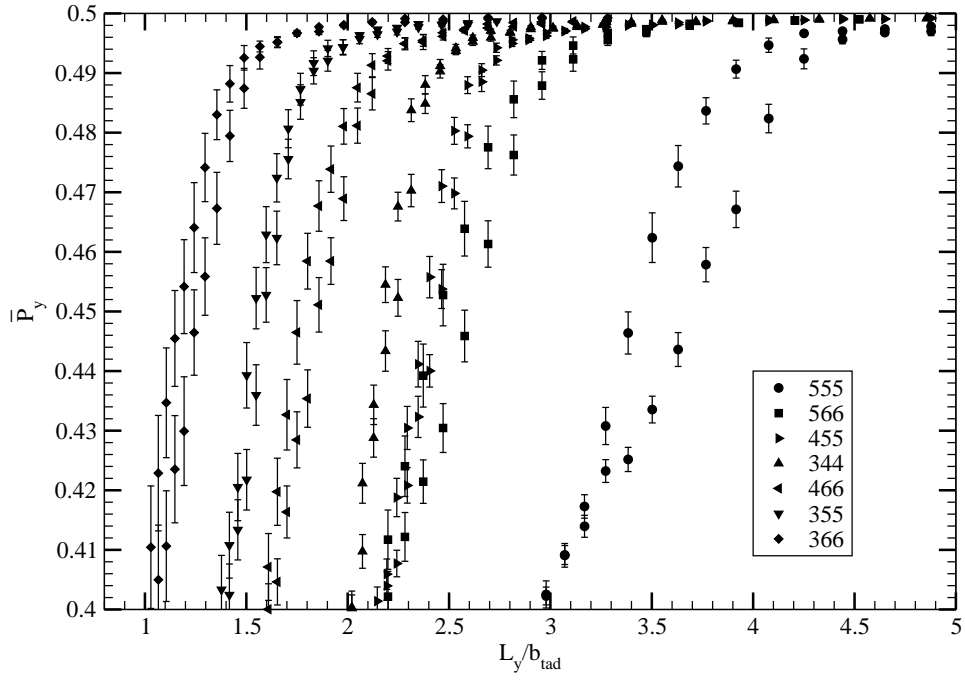


Figure 5: Plot of \bar{P}_y showing the 1c-2c transition on lattices with $L_x \leq L_y$.

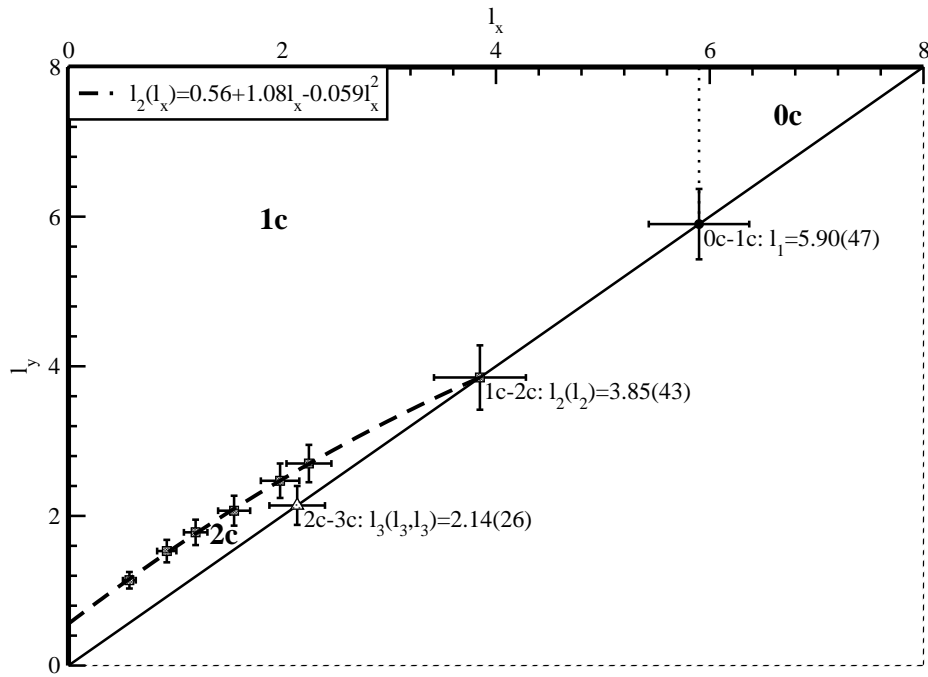


Figure 6: Phase diagram for $l_x \leq l_y \leq l_z$